Proceedings of the EuroGNC 2013, 2nd CEAS Specialist Conference on
Guidance, Navigation & Control, Delft University of Technology, Delft,
The Netherlands, April 10-12, 2013

Decentralized Energy Management for Spacecraft Attitude Determination

Rouzbeh Amini, Eberhard Gill and Georgi Gaydadjiev

Abstract Employment of wireless links for spacecraft onboard data communication provides promising solutions for improved modularity of onboard system architectures. In such onboard wireless network infrastructure power is highly distributed and often limited for some of the nodes that makes energy efficient data collection extremely important. Wireless technology can be specifically employed for sensors and actuators of attitude determination and control system (ADCS). In this paper we propose a new decentralized architectural scheme for energy management of onboard wireless sensors and actuators network (OWSAN). Our energy manager is based on a decentralized sensor scheduling. The local node energy managers dynamically schedule the sleep periods of wireless transmitters to lower the frequency of data communication activities which, as a consequence, reduces the energy consumption and minimizes the chances of communication collisions among the wireless nodes. The results of the simulation show about 25% to 33% reduction in wireless communication activities of some nodes without sacrificing the ADCS accuracy which implies a significant improvement in sensors energy efficiency.

Rouzbeh Amini
Space Systems Engineering, Delft University of Technology, Delft, The Netherlands,
e-mail: R.Amini@tudelft.nl

Eberhard Gill
Space Systems Engineering, Delft University of Technology, Delft, The Netherlands,
e-mail: E.K.A.Gill@tudelft.nl

Georgi Gaydadjiev
Computer Science and Engineering department, Chalmers University, Gothenburg, Sweden,
e-mail: georgig@chalmers.se

1 Introduction

Recently, applying novel technologies and advanced electronics have enabled a more modular and reconfigurable design for spacecraft onboard hardware architectures. Among these new technologies, onboard wireless communication between spacecraft subsystems is very promising and allows design flexibility and mass reduction. Moreover, it improves the autonomy, ease of system integration and testing. Enabling onboard wireless data communication can alleviate other issues of wired communication such as failures of wires and connectors, high cost of late design changes, time overhead for allocating routes and shields, undesired ground loops, etc. There are numerous technical challenges related to this new technology. Restricted onboard energy budget is one of the major challenges to overcome.

In our previous work we introduced properties of spacecraft onboard wireless sensors and actuators network (OWSAN) [3]. We also defined a set of typical requirements in respect to the wireless data handling system for small satellites. We concluded that OWSAN shows different characteristics comparing to typical sensor networks due to its specific application. It was shown that not every onboard subsystem is an appropriate candidate for being equipped with a wireless transmitter. Our evaluation showed that sensors of attitude determination and control system (ADCS) are potential candidates to use low power wireless data transmission technologies such as ZigBee or other derivatives of IEEE 802.15.4 standard. This is due to the low to medium measurement data rates of ADCS sensors (typically around 1 Hz) and relatively relaxed requirements on data robustness. Several studies on energy efficiency of wireless sensor networks have shown that a wireless transceiver is the part responsible for the consumption of the most energy on a sensor node and any attempt to decrease the energy consumption of this part yields sensible benefits in the overal energy efficiency. In fact with new developments in ultra low power processors, onboard communication can be safely traded for onboard computation [11]. The core idea of our solution is to adjust sampling rates of ADCS sensors when the satellite is not performing high precision maneuvers and ideally arrive to a *sampling on demand* architecture. A reduced sampling rate naturally lowers the need for frequent wireless transmission and ultimately saves energy on sensor nodes and thus the entire system.

Some prototypes of wireless ADCS sensors are already designed and tested [4, 6, 17]. These devices are usually composed of a sensor which is integrated with a micro-controller, battery, an energy harvesting solution and a wireless transmitter. To guarantee the nominal operation of such onboard sensors, energy efficiency should be considered by in the electronics, communication standard, sensing instrument and the software. However wireless transmission needs more care because it consumes more energy compared to sensing and onboard computation. Therefore it is very convenient to use additional onboard processing on the sensor to reduce the wireless transmission. An onboard energy management scheme can reduce the energy consumption and improve the life time of a sensor. Different approaches to implement energy managers have been introduced in literature. Some of the techniques rely on approximate querying which exploits the natural trade-off between

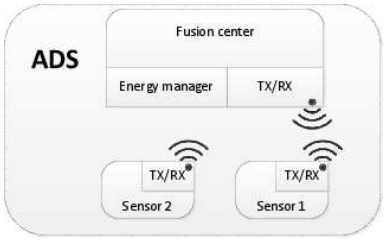

Fig. 1 In centralized scheme, the energy manager is resided in the fusion center which globally tunes and schedules the sampling rate of sensors.

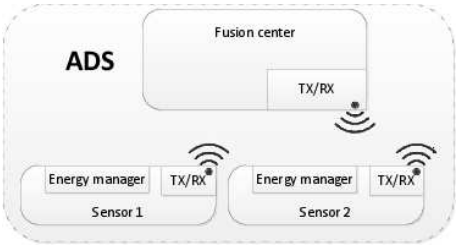

Fig. 2 This scheme shows decentralized energy management for OWSAN. In this architecture, each node is equipped with a local energy manager which regulates the activities of that node.

energy consumption and data accuracy [14, 13, 15]. This category of techniques basically relies on the application-specific error bounds which are disseminated to each sensor node along with the query. A measurement is sent to the base station if the change of two consecutive sensor values exceeds a user-defined error bound. There are also other approaches which use sleep scheduling but they mostly lack the explicit interaction with the application layer modules [9, 12]. Most of these approaches are not suitable for an onboard network of sensors where the dynamics of the spacecraft system is known.

We believe that the application constraints play a great role in designing a more efficient energy management mechanism specifically for sensors of spacecraft ADCS because the sensor measurements are highly correlated and can be predicted. In our previous work, we introduced a centralized energy management scheme based on centralized measurement fusion (see Fig. 1). The energy manager uses optimal estimations of sensor measurements and dynamically schedules the operation mode of the sensors by changing their sampling frequency [3]. This approach ensures a very small computation overhead on the sensor nodes of OWSAN, because no preprocessing or decision making is necessary on sensor nodes. But it decreases the modularity and scalability of the architecture.

In this paper we suggest a decentralized architecture for energy management of OWSAN. Comparing Fig. 1 with Fig. 2 clarifies the difference of the new architecture. Each sensor node is equipped with adequate onboard processing power to decide and schedule its own transmission activities. This new system architecture introduces a number of advantages compared to the centralized design:

- Improving system reliability by decentralizing the decision making. Therefore the fusion center is no longer a critical single point of failure;
- Increasing the architecture flexibility and scalability;
- Increasing the modularity of the design;

- Providing system scalability;
- Providing robustness to ADCS in case of a sensor failure.

The rest of this paper is organized as follows: Sect. 2 provides overview of the concept is given while the details of the design are described in Sect. 3. The mathematical model of the architecture is provided in Sect. 4, finally in Sect. 5 the performance of the design is tested and proved.

2 Onboard wireless network

In a fully modular onboard wireless network, sensor nodes are required to operate on limited energy budgets. Energy management can prolong the lifetime of a sensor network and conserve scarce energy resources. However, inefficient management could result in severe performance degradation. In this work, we study onboard attitude determination system which is composed of wireless sensor nodes and a fusion center (onboard computer). Each sensor node uses a local energy harvesting and storage unit and it has limited available energy. The fusion center represents a node as well with free access to energy. The onboard wireless sensor nodes in our study are a 3-axis gyro, a 3-axis magnetometer and a sun-sensor.

The goal of energy manager on each node is to reduce the energy consumption of the same node by increasing the sleep period of wireless transmitter. A component level design for sensors scheduling can contribute to this goal by reducing the wireless communication frequency of the sensor nodes. The energy management scheme is a decision making technique which can be implemented either centralized in the fusion center or decentralized.

In the decentralized form, each sensor node schedules the time to establish a new communication with central fusion. Therefore the wireless transmitter on the node can be switched off or put in the sleep mode while a transmission is not required. As soon as a new communication is mandatory, the sensor node wakes up its local transmitter and submits the latest local measurement vector. During this communication window, the sensor may receive the latest updates about the spacecraft status, and other global information which is locally required to schedule the next communication. This information can be simply measurement vectors made by other sensor nodes. This scheduling approach is very suitable for ADCS due to slow dynamics of spacecraft. Abrupt changes are not typically seen in ADCS sensors measurements and the spacecraft state is predictable.

2.1 Communication standard

The features of communication standard plays a major rule in designing the architecture. It provides the tool to implement the scheduling scheme. In our previous work we have already concluded that the family of standards based on IEEE 802.15.4 are

very convenient for OWSAN [2]. Therefore the proposed architecture is based on employing a beacon-enabled mesh network such as ZigBee. This means that nodes of the onboard network can only transmit inside of a predetermined time slot. In beacon-enabled network, the network coordinator will periodically generate a super frame which is identified as a beacon frame. In OWSAN it is very practical to assume that onboard computer is the network coordinator. the emission of the super frame implies the use of time slots, every node must synchronize with the super frame in the time domain. Each node is assigned a specific time slot that it can use to transmit and receive data. A node will synchronize with the ZigBee coordinator's beacons and wakes up just before the beacon is to be generated. Then it performs its action inside the active time period and then goes back to sleep mode [5]. These properties are very suitable for designing a decentralized energy management scheme for spacecraft ADCS.

3 Onboard decentralized architecture

To exploit the benefits of a decentralized architecture, different configuration can be employed. In one configuration sensors directly communicate to each other. This configuration can be very energy exhaustive because it naturally decreases the sleep period of the local wireless transmitters. Also this configuration does not take benefit of the availability of spacecraft onboard computer (OBC) as a node without severe energy constraints. In second configuration, the communication between sensors is established through the onboard computer. Here OBC contributes as a relay or buffer to distributes the information between nodes and provide the network beacon. It waits to receive a request from a node and only then it transmits the latest measurements vector or its best available estimate. Obviously any other node can substitute OBC which increases the robustness. Also it is very convenient to accommodate attitude determination algorithm on OBC to maintain a global estimate of spacecraft attitude. This enables OBC to provide extra information about spacecraft attitude to the nodes. As a result, the onboard computer always holds the latest measurements available from the nodes. Nevertheless, the actual latest measurements can be from different time instances or can be revised according to the dynamics of the system. Thus, each sensor node has enough information about the status of the attitude determination and can decide whether its local measurement vector can be communicated at a lower frequency to the other nodes. Figure 3 shows different components in a sensor node to facilitate implementation of the described scheme. Such architecture shows the following advantages:

- Local estimates available in the sensor can be used for local decision making;
- The communication cost can be reduced by transmitting only when measurements are necessary;
- A distributed architecture can have further survivability in the event that the central unit fails;
- The computation load of the central unit can be reduced.

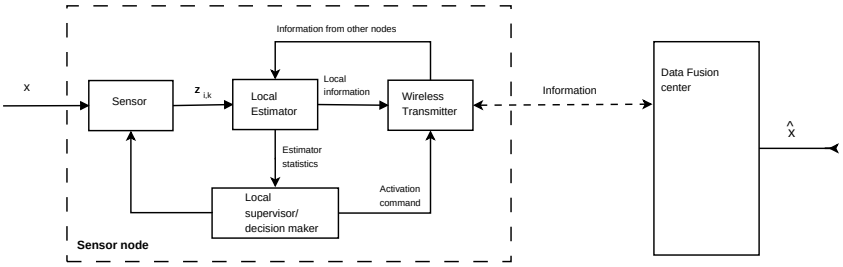

Fig. 3 Structure of a sensor node in a decentralized architecture with local estimator and decision maker.

Practically this decentralized configuration can be realized by implementing information filters in federated form. Being equivalent to the Kalman filter algebraically, the information filter is easier to decentralize, initialize, and fuse than a Kalman filter based fusion. The next section will formulate this idea.

4 Problem formulation

The solution to attitude determination of spacecraft with difference measurement vectors from sensors can be approached by building a state estimation algorithm based on Kalman filtering.

4.1 Kalman filter

For a system with linear process and observations models, a direct and close form for Kalman filter can be derived. Linear state space formulation for such system with state vector $\mathbf{x}_{n\times 1}$ and sensor measurement vector $\mathbf{z}_{m\times 1}$ in discrete form is

$$\begin{cases} \mathbf{x}(t_k) = \mathbf{F}(t_{k-1})\mathbf{x}(t_{k-1}) + \mathbf{v}(t_{k-1}) \\ \mathbf{z}(t_k) = \mathbf{H}(t_k)\mathbf{x}(t_k) + \mathbf{w}(t_k) \end{cases} \tag{1}$$

here $\mathbf{F}(t_k)$ is a $n \times n$ matrix, $\mathbf{H}(t_k)$ is a $m \times n$ measurement matrix. $\mathbf{v}$ and $\mathbf{w}$ are white noise vectors for process model and measurements. The noise vectors are assumed to have Gaussian distribution with known properties. For this system, Algorithm 1 summarizes linear Kalman filtering algorithm.

Algorithm 1 Standard Kalman filter algorithm. Here $\mathbf{P}$ is the error covariance matrix, $\mathbf{K}$ is the Kalman filter gain, $\mathbf{S}$ is the innovations covariance matrix, $\mathbf{Q}$ is the covariance matrix of process noise and $\mathbf{R}$ is the covariance matrix of the measurement noise.

1. Initialization:
$$\hat{\mathbf{x}}(t_0) = \mathbf{x}_0, \quad \mathbf{P}(t_0) = \mathbf{P}_0$$
2. Time update:
   2.1. Project the system state ahead:
$$\hat{\mathbf{x}}_{k|k-1}(t_k) = \mathbf{F}(t_{k-1})\hat{\mathbf{x}}_{k|k}(t_{k-1})$$
   2.2. Project the error covariance ahead:
$$\mathbf{P}_{k|k-1}(t_k) = \mathbf{F}(t_{k-1})\mathbf{P}_{k-1|k-1}(t_{k-1})\mathbf{F}(t_{k-1})^T + \mathbf{Q}(t_{k-1})$$
3. Measurement update:
   3.1. Compute the innovations:
$$\varepsilon(t_k) = \mathbf{z}(t_k) - \mathbf{H}(t_k)\hat{\mathbf{x}}_{k|k-1}(t_k)$$
$$\mathbf{S}(t_k) = \mathbf{H}(t_k)\mathbf{P}_{k|k-1}(t_k)\mathbf{H}^T(t_k) + \mathbf{R}(t_k)$$
   3.2. Compute the Kalman filter gain:
$$\mathbf{K}(t_k) = \mathbf{P}_{k|k-1}(t_k)\mathbf{H}^T(t_k)\mathbf{S}^{-1}(t_k)$$
   3.3. Update the state estimate with measurement $\mathbf{z}_(t_k)$:
$$\hat{\mathbf{x}}_{k|k}(t_k) = \hat{\mathbf{x}}_{k|k-1}(t_k) + \mathbf{K}(t_k)\varepsilon(t_k)$$
   3.4. Update the error covariance matrix:
$$\mathbf{P}_{k|k}(t_k) = \mathbf{P}_{k|k-1}(t_k) - \mathbf{P}_{k|k-1}(t_k)\mathbf{K}(t_k)\mathbf{H}(t_k)$$

4.2 Information filter

Kalman filter equations can be converted to *information filter* form which provides numerical advantages for a decentralized architecture. The term information here is applied in the *Fisher* sense and the formulation is expressed in term of the information measure about the states of the system rather than the direct state estimation and its covariance. The formulation is based on reformulation of Kalman filter using the following defined variables

$$\begin{cases} \mathbf{Y}_{k_1|k_2}(t_k) := \mathbf{P}^{-1}_{k_1|k_2}(t_k) \\ \hat{\mathbf{y}}_{k_1|k_2}(t_k) := \mathbf{P}^{-1}_{k_1|k_2}(t_k)\hat{\mathbf{x}}_{k_1|k_2}(t_k) \\ \mathbf{i}(t_k) := \mathbf{H}^T(t_k)\mathbf{R}^{-1}(t_k)\mathbf{z}(t_k) \\ \mathbf{I}(t_k) := \mathbf{H}^T(t_k)\mathbf{R}^{-1}(t_k)\mathbf{H}(t_k) \end{cases} . \tag{2}$$

In this formulation $\hat{\mathbf{y}}_{k_1|k_2}$ is called *information state vector,* $\mathbf{Y}_{k_1|k_2}$ is *information matrix*, $\mathbf{i}$ is *information state contribution* from an observation $\mathbf{z}$ and $\mathbf{I}$ is its *associated information matrix*. With these definitions, linear information filter is shown by Algorithm 2.

By observing Algorithm 2, we understand that the correction equations of information filter is computationally easier than that of Kalman filter. This property can be used later in decentralizing the data fusion. Also it can be seen that there is no gain and innovation covariance matrix involved in the computation. Also unlike the

Algorithm 2 Standard Information filter algorithm

1. Initialization:
$$\mathbf{Y}(t_0) = \mathbf{P}_0^{-1}, \quad \hat{\mathbf{y}}(t_0) = \mathbf{Y}(t_0)\mathbf{x}_0$$
2. Prediction:
   2.1. Project the information state vector:
$$\hat{\mathbf{y}}_{k|k-1}(t_k) = \mathbf{Y}_{k|k-1}(t_k)\mathbf{F}(t_{k-1})\mathbf{Y}^{-1}_{k-1|k-1}(t_{k-1})\hat{\mathbf{y}}_{k-1|k-1}(t_{k-1})$$
   2.2. Project the information matrix:
$$\mathbf{Y}_{k|k-1}(t_k) = \left(\mathbf{F}(t_{k-1})\mathbf{Y}^{-1}_{k-1|k-1}(t_k)\mathbf{F}^T(t_k) + \mathbf{Q}(t_k)\right)^{-1}$$
3. Correction:
   3.1. Compute the information state update:
$$\hat{\mathbf{y}}_{k|k}(t_k) = \hat{\mathbf{y}}_{k|k-1}(t_k) + \mathbf{i}(t_k)$$
   3.2. Compute the information matrix update:
$$\mathbf{Y}_{k|k}(t_k) = \mathbf{Y}_{k|k-1}(t_k) + \mathbf{I}(t_k)$$

Kalman filter, the initial condition for the information state vector and information matrix can be set to zero information which in practice can be a diagonal matrix with small non-zero diagonal elements.

4.3 Decentralized Information filter

Consider the scheme presented in Figure 4. Each node generates its own observation vector and also computes its local prediction of the process model. Therefore the information from observation $\mathbf{z}_i(t_k)$ and its associated information matrix for node *i* are known. According to (2) on node *i* we have

$$\mathbf{i}_i(t_k) = \mathbf{H}_i^T(t_k)\mathbf{R}_i^{-1}(t_k)\mathbf{z}_i(t_k) \tag{3}$$
$$\mathbf{I}_i(t_k) = \mathbf{H}_i^T(t_k)\mathbf{R}_i^{-1}(t_k)\mathbf{H}_i(t_k) \quad . \tag{4}$$

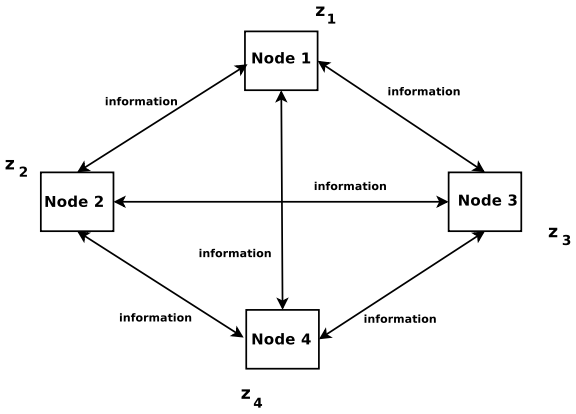

Fig. 4 Decentralized scheme for OWSAN with two way communication channels and interconnected nodes.

The prediction formulas for node i will be

$$\hat{\mathbf{y}}_{i,k|k-1}(t_k) = \mathbf{L}_{i,k|k-1}(t_k)\hat{\mathbf{y}}_{i,k|k-1}(t_{k-1}) \tag{5}$$

$$\mathbf{Y}_{i,k|k-1}(t_k) = \left(\mathbf{F}(t_{k-1})\mathbf{Y}^{-1}_{i,k-1|k-1}(t_k)\mathbf{F}^T(t_{k-1}) + \mathbf{Q}(t_k)\right)^{-1} \tag{6}$$

with $\mathbf{L}_{i,k|k-1}$ being the local propagation coefficient defined as

$$\mathbf{L}_{i,k|k-1}(t_k) = \mathbf{Y}_{i,k|k-1}(t_k)\mathbf{F}(t_{k-1})\mathbf{Y}^{-1}_{i,k|k-1}(t_{k-1}) \tag{7}$$

which is independent from all local observations. At this point, the *local partial correction* of the information state vector on node i can be immediately found by using the third step of Algorithm 2. It is called local partial correction because it can be further improved by providing the information communicated from all other nodes. If there is no information received from a node, the related information will be simply replaced by zero. The local partial correction for node i is

$$\check{\mathbf{y}}_{i,k|k} = \hat{\mathbf{y}}_{i,k|k-1}(t_k) + \mathbf{i}_i(t_k) \tag{8}$$

$$\check{\mathbf{Y}}_{i,k|k} = \mathbf{Y}_{i,k|k-1}(t_k) + \mathbf{I}_i(t_k) \quad . \tag{9}$$

After sharing all local partial corrections between nodes the final local correction on node i becomes

$$\hat{\mathbf{y}}_{i,k|k}(t_k) = \hat{\mathbf{y}}_{i,k|k-1}(t_k) + \sum_{j=1}^{M}\left(\check{\mathbf{y}}_{j,k|k}(t_k) - \hat{\mathbf{y}}_{i,k|k-1}(t_k)\right) \tag{10}$$

$$\mathbf{Y}_{i,k|k}(t_k) = \mathbf{Y}_{i,k|k-1}(t_k) + \sum_{j=1}^{M}\left(\check{\mathbf{Y}}_{j,k|k}(t_k) - \mathbf{Y}_{i,k|k-1}(t_k)\right) \tag{11}$$

The same methodology can be used to derive the results when the process model is not linear. In this case the local predictions can be calculated by

$$\hat{\mathbf{y}}_{i,k|k-1}(t_k) = \mathbf{Y}_{i,k|k-1}(t_k)\mathbf{f}(\hat{\mathbf{x}}_{i,k-1|k-1}(t_{k-1})) \tag{12}$$

$$\mathbf{Y}_{i,k|k-1}(t_k) = \left(\boldsymbol{\Phi}\left(\hat{\mathbf{x}}_{i,k-1|k-1}(t_{k-1})\right)\mathbf{Y}^{-1}_{i,k-1|k-1}(t_k)\boldsymbol{\Phi}^T(\hat{\mathbf{x}}_{i,k-1|k-1}(t_{k-1})) + \mathbf{Q}(t_k)\right)^{-1} \tag{13}$$

The local partial correction equations are similar to (10) and (11), respectively. Also the final correction equations can be calculated by (8) and (9). However, the local information parameters will change into

$$\mathbf{I}_i(t_k) = \Upsilon_i^T\left(\hat{\mathbf{x}}_{i,k|k-1}(t_k)\right)\mathbf{R}^{-1}(t_k)\Upsilon_i(t_k) \tag{14}$$

$$\mathbf{i}_i(t_k) = \Upsilon_i^T\left(\hat{\mathbf{x}}_{i,k|k-1}(t_k)\right)\mathbf{R}^{-1}(t_k)\left(\varepsilon_i(t_k) + \Upsilon_i\left(\hat{\mathbf{x}}_{i,k|k-1}(t_k)\right)\hat{\mathbf{x}}_{i,k|k-1}(t_k)\right) \tag{15}$$

where $\boldsymbol{\Phi}$ and Υ are Jacobian matrices for process and measurements model, similar to the formulation of extended Kalman filter [8].

$$\varepsilon_i(t_k) = \mathbf{z}_i(t_k) - \mathbf{h}_i\left(\hat{\mathbf{x}}_{i,k|k-1}(t_k)\right) \quad . \tag{16}$$

4.4 Energy manager

We design the energy manager based on a property of estimation algorithm which was described before. It can be shown that the measurements innovation vector $\varepsilon(t_k)$ and state estimate error are both Gaussian random processes with zero mean. Therefore the following normalized quadratic functions have χ^2 distribution

$$\mathbf{N}_\varepsilon(t_k) = \varepsilon^T(t_k)\mathbf{S}^{-1}(t_k)\varepsilon(t_k) \tag{17}$$

$$\mathbf{N}_{\tilde{\mathbf{x}}}(t_k) = \left(\mathbf{x}(t_k) - \hat{\mathbf{x}}_{k|k}(t_k)\right)^T \mathbf{P}^T_{k|k}(t_k)\left(\mathbf{x}(t_k) - \hat{\mathbf{x}}_{k|k}(t_k)\right) \quad . \tag{18}$$

$\mathbf{N}_\varepsilon(t_k)$ is an indication for the inconsistency of the measurements and has m degrees of freedom with m being the number of the independent measurements, while $\mathbf{N}_{\tilde{\mathbf{x}}}(t_k)$ is a measure of the uncertainty level in estimating the states and has n degrees of freedom with n being the number of the states. We can use this stochastic property of the innovation vector in combination with a decision maker to decide if a new measurement vector is required locally to maintain the attitude estimation performance or not. For this purpose, a decision maker based on hypotheses tests can be employed. For our application, hypothesis H_0 can be "the filter operation is satisfactory" and hypothesis H_1 is "the filter operation is not satisfactory". The result of type I test error is a false alarm (FA) resulting in requesting for new sensor measurements. The result of type II error will be a missed alarm (MA) which causes an increase in the error of the Kalman estimation. To lower the energy consumption it is desired to make sure that the probability of occurrence of type I error is as low as possible. We have

$$P_{FA} = P(H_1|H_0) = \int_{\aleph_1} p(\zeta|H_0)\,\mathrm{d}\zeta \tag{19}$$

$$P_{MA} = P(H_0|H_1) = \int_{\aleph_0} p(\zeta|H_1)\,\mathrm{d}\zeta \tag{20}$$

where ζ is representing a test statistics and $p(\zeta|H_0)$ is its conditional probability density. The set $\aleph_0$ is a region containing ζ while hypothesis H_1 holds true. Similarly, set $\aleph_1$ is a region containing ζ while hypothesis H_0 holds true. Sets $\aleph_0$ and $\aleph_1$ partition the observation space together. Also it can be seen that

$$P_D = P(H_1|H_1) = \int_{\aleph_1} p(\zeta|H_1)\,\mathrm{d}\zeta = 1 - P_{FA} \tag{21}$$

A good decision making algorithm should be able to minimize a wrong decision in both cases which is

$$P_E = P_0 P_{FA} + P_1 P_{MA} \tag{22}$$

where P_E is the probability of making an erroneous decision, P_0 is the probability that hypotheses H_0 occurs and P_1 is the probability of H_1 occurrence. From energy efficiency view, P_{FA} in more expensive for the system, therefore a good decision making system should provide a solution to lower the probability of requesting unnecessary measurements. The concept of *confidence interval* is often used which is the probability that a test statistics falls in a known region, and is usually indicated with a certain percentage. For the associated range of a given confidence interval a threshold τ can be defined such that

$$P_{FA}(\tau) = \eta \tag{23}$$

here η is expressed as a percentage and denotes the significance level. Then the confidence level becomes $1-\eta$. Therefore a smaller significance level results in a bigger threshold for the hypothesis tests in (19).

In OWSAN data fusion, the occurrence probability of either hypotheses are not known beforehand. In such case we can use Neyman-Pearson decision making method. The goal is to maximize P_D for an arbitrary probability of P_{FA}. To obtain a trade-off between P_{FA} and P_{MA} we can try to minimize the following cost function

$$F = P_{MA} + \tau(P_{FA} - \eta) = \tau(1-\eta) + \int_{\aleph_0} \big(p(\zeta|H_1) - \tau(\zeta|H_0)\big)\,\mathrm{d}\zeta \tag{24}$$

with $\tau \geq 0$ being the Lagrange modifier. The result of minimization and applying the likelihood ratio test leads to the Neyman-Pearson hypotheses test as follows

$$V(\zeta) = \frac{p(\zeta|H_1)}{p(\zeta|H_0)} \underset{H_0}{\overset{H_1}{\gtrless}} \tau \tag{25}$$

The threshold is the Lagrange multiplier τ which is chosen such that satisfies the significance level η

$$P_{FA} = \int_{\aleph_1} p(\zeta|H_0)\,\mathrm{d}\zeta = \int_{\tau}^{\infty} p(\zeta|H_0)\,\mathrm{d}\zeta = \eta \tag{26}$$

We can apply this decision making rule to the measurement innovations or state estimate errors to decide about the necessity of a new measurement vector from a specific sensor node. To enable this, we need to identify the probability density function $p(\zeta)$ for hypotheses H_0 and H_1. This will enable decision making in the local level and global level for both centralized and decentralized architecture. For example, we consider a sequence of one dimensional n residuals of local Kalman filter on one of OWSAN nodes. This sequence has Gaussian distribution with unknown mean μ but known variance σ^2. μ can be either equal to μ_0 (hypothesis H_0) or μ_1 (hypothesis H_1), and $\mu_1 > \mu_0$. The likelihood of the observation is

$$p(\zeta|\mu) = \prod_i \frac{1}{\sqrt{2\pi}\sigma} \exp(-\frac{(\zeta_i-\mu)^2}{2\sigma^2}) = \frac{1}{(\sqrt{2\pi})^n\sigma^n} \exp(-\frac{\sum_i(\zeta_i-\mu)^2}{2\sigma^2})$$
$$= \frac{1}{(\sqrt{2\pi})^n\sigma^n} \exp(-\frac{n\mu^2}{2\sigma^2}) \exp(-\frac{n\mu\bar{\zeta}}{2\sigma^2}) \exp(-\frac{\sum_i \zeta_i}{2\sigma^2}) \quad (27)$$

The ratio of likelihood from Neyman Pearson test is

$$V(\zeta) = \frac{p(\zeta|\mu_1)}{p(\zeta|\mu_0)} = K \exp(\frac{n(\mu_1-\mu_0)\bar{\zeta}}{\sigma^2}) \quad (28)$$

where $\bar{\zeta}$ is the mean of ζ. According to Neyman-Pearson, H_0 should be rejected if the following condition holds

$$\exp(\frac{n(\mu_1-\mu_0)\bar{\zeta}}{\sigma^2}) > \tau \quad (29)$$

4.5 Dealing with missing measurements

By operating the described energy manager on each node, the local estimators will not receive measurement vectors at full rate, therefore the estimator will become suboptimal. This is inevitable and can question the stability of the Kalman filter (or information filter). This phenomena is similar to the problem studied by Faridani [7] and Sinopoli *et al.* [16] and is addressed by Liu and Goldsmith [10]. Liu and Goldsmith have calculated an upper and lower bound for the transmission rate of the measurements which guarantees the stability of the estimator.

4.6 Decentralized energy manager

We consider a system with only two sensor nodes and OBC as the relay and buffer. On the sensor node 1, local measurements are generated with the nominal sampling rate $f_{1,1}$ and immediately communicated to OBC and node 2. The local estimator on node 1 maintains a global model of the system and all system statistics and according to (10) and (11). parameters up to time t_k. Therefore it can compute a local prediction of spacecraft states at time t_k with its error covariance matrix which are $\hat{\mathbf{x}}_{i,k|k-1}(t_k)$ and $\mathbf{P}_{i,k|k-1}(t_k)$. Furthermore, it can predict its own observation vector $\hat{\mathbf{z}}_{1,k|k-1}(t_k)$ and node 2's observation vector $\hat{\mathbf{z}}_{2,k|k-1}$. Also it can compute its own local partial information state vector $\check{\mathbf{y}}_{1,k|k}$ and its information matrix $\check{\mathbf{Y}}_{1,k|k-1}$. Each node runs a local energy management algorithm. In this scheme, the local energy manager on node 1 is only concerned about reducing the sampling rate of sensor 1. It uses a decision maker based on hypothesis tests to evaluate possibility of reducing the sampling rate of the sensor by evaluating the statistical properties of its local

Algorithm 3 Decentralized energy manager algorithm

1. Initialization:

$\hat{\mathbf{x}}(t_0) = \mathbf{x}_0, \quad \mathbf{P}(t_0) = \mathbf{P}_0, \quad \gamma_{k,i} = 1 \quad f_i = f_{i,1}, \quad \check{\mathbf{z}}(t_0) = \mathbf{z}_0, \quad \mathbf{R}_i(t_0) = \mathbf{R}_{i,0}$

$H_0 =$ ADCS estimation is accurate enough;

$H_1 =$ ADCS estimation is not accurate enough;

2. Prediction:

2.1. Project the system state and information state ahead:

$\hat{\mathbf{x}}_{k|k-1}(t_k) = \mathbf{F}(t_{k-1})\hat{\mathbf{x}}_{k|k}(t_{k-1});$

$\hat{\mathbf{y}}_{i,k|k-1}(t_k) = \mathbf{L}_{i,k|k-1}(t_k)\hat{\mathbf{y}}_{i,k|k-1}(t_{k-1});$

2.2. Project the error covariance and information matrix ahead:

$\mathbf{P}_{k|k-1}(t_k) = \mathbf{F}(t_{k-1})\mathbf{P}_{k-1|k-1}(t_{k-1})\mathbf{F}(t_{k-1})^T + \mathbf{Q}(t_{k-1});$

$\mathbf{Y}_{i,k|k-1}(t_k) = \left(\mathbf{F}(t_{k-1})\mathbf{Y}^{-1}_{i,k-1|k-1}(t_k)\mathbf{F}^T(t_{k-1}) + \mathbf{Q}(t_k)\right)^{-1}$

2.3. Project the sensor measurement of the local sensor ahead:

$\hat{\mathbf{z}}_{i,k|k-1}(t_k) = \mathbf{H}_i(t_k)\hat{\mathbf{x}}_{k|k-1}(t_k);$

3. Decision making and correction:

3.1. If sensor observation vector $\mathbf{z}_{i,k}(t_k)$ is available set $\gamma_{i,k} = 1$ and:

3.1.1. Compute the innovation vector and its covariance:

$\varepsilon_i(t_k) = \mathbf{z}_i(t_k) - \hat{\mathbf{z}}_{k|k-1}(t_k);$

$\mathbf{S}_i(t_k) = \mathbf{H}_i(t_k)\mathbf{P}_{k|k-1}(t_k)\mathbf{H}_i^T(t_k) + \mathbf{R}_i(t_k).$

3.1.2. Run decision maker test and accept H_0 or H_1:

$$V_{i,k}(\zeta) = \frac{p(\zeta_i|H_1)}{p(\zeta_i|H_0)} \underset{H_0}{\overset{H_1}{\gtrless}} \tau$$

3.1.3. Determine the sampling rate for the sensor:

$$f_i = \begin{cases} f_{i,1} \text{ , if } H_0 \text{ is true;} \\ f_{i,2} \text{ , if } H_1 \text{ is true.} \end{cases}$$

3.1.4. Compute information of the the new measurement:

$\mathbf{i}_i(t_k) = \mathbf{H}_i^T(t_k)\mathbf{R}_i^{-1}(t_k)\mathbf{z}_i(t_k)$

$\mathbf{I}_i(t_k) = \mathbf{H}_i^T(t_k)\mathbf{R}_i^{-1}(t_k)\mathbf{H}_i(t_k)$

3.2. If sensor observation vector $\mathbf{z}_{i,k}(t_k)$ is NOT available:

$\mathbf{i}_i(t_k) = \mathbf{0} \quad , \quad \mathbf{I}_i(t_k) = \mathbf{0};$

3.3. Compute the local partial corrections (see (8) and (9)):

$\check{\mathbf{y}}_{i,k|k} = \hat{\mathbf{y}}_{i,k|k-1}(t_k) + \mathbf{i}_i(t_k)$

$\check{\mathbf{Y}}_{i,k|k} = \mathbf{Y}_{i,k|k-1}(t_k) + \mathbf{I}_i(t_k)$

3.4. Interchange the the local partial corrections with other nodes

3.5. Compute the final local correction:

$\hat{\mathbf{y}}_{i,k|k}(t_k) = \hat{\mathbf{y}}_{i,k|k-1}(t_k) + \sum_{j=1}^{M}\left(\check{\mathbf{y}}_{j,k|k}(t_k) - \hat{\mathbf{y}}_{i,k|k-1}(t_k)\right)$

$\mathbf{Y}_{i,k|k}(t_k) = \mathbf{Y}_{i,k|k-1}(t_k) + \sum_{j=1}^{M}\left(\check{\mathbf{Y}}_{j,k|k}(t_k) - \mathbf{Y}_{i,k|k-1}(t_k)\right)$

measurements. Algorithm 3 presents the operation of decentralized energy manager on an OWSAN node .

Table 1 Simulation parameters for benchmark pointing scenario.

Parameter	Value	Unit
Simulation step	$T_s = 1$	[second]
Inertia tensor	$\underline{\mathbf{I}} = \begin{pmatrix} 0.002 & 0 & 0 \\ 0 & 0.002 & 0 \\ 0 & 0 & 0.002 \end{pmatrix}$	[kg/meter^2]
Initial rotation rate	$\omega = \begin{pmatrix} 0.01 \\ -0.01 \\ 0.01 \end{pmatrix}$	[rad/second]
Initial attitude	$\mathbf{q}_0 = \begin{pmatrix} 0 \\ 0 \\ 0 \\ 1 \end{pmatrix}^T$	-
Target attitude (pointing scenario)	$\mathbf{q}_{\text{set}} = \begin{pmatrix} 0.4496 \\ 0.2375 \\ 0.1692 \\ 0.8463 \end{pmatrix}$	-

5 Experimental results

The simulations are carried on by SpaceTool simulation environment which is a Matlab/Simulink toolbox. Design and development of this toolbox was initiated in 2003 as a simulation tool for AAUSAT-II CubeSat in Aalborg university [1]. Later on the toolbox design was revisited and extended in the context of the MicroNED MISAT project at Aerospace Engineering faculty of Delft University of Technology. Previous generations of this tool were used in design and development of AAUSAT-II and Delfi-C3 CubeSats. Validity of the majority of the models were internally verified against EuroSim designed by Dutch Space BV and Spacecraft Control Toolbox (SCT) developed by Princeton Satellite Systems.

We assumed a simulation scenario based on a small CubeSat size spacecraft in LEO orbit. The minimum required ADCS precision is chosen as 0.5 degree (absolute error). The simulation is ran while the spacecraft is out of eclipse. The performance of proposed decentralized energy manager is tested in a pointing scenario, where the spacecraft shall point at a specific direction. The designed maneuver represents a $(30^\circ - 15^\circ - 60^\circ)$ rotation. A linear-quadratic regulator (LQR) is designed to control the attitude with aid of a set of three reaction wheels. The aim is to maintain the performance of attitude determination and reduce wireless transmission activity. For this simulation, we consider a set of a 3-axis gyroscope, 3-axis magnetometer and six sun sensors as ADCS sensors. The models of the sensors are generic. For the magnetometer, an accuracy of $10nT$ with noise level of $100pT/\sqrt{Hz}$ is accounted for simulations. The sun sensor accuracy is assumed to be better than 0.03 degree and the gyro noise level is chosen to be 10^{-5}. These assumptions are close to those of state-of-art sensors which are commonly used in small spacecraft.

Table 2 Attitude estimation results in pointing scenario without energy manager. Subscripts *y*, *p* and *r* refer to yaw, pitch and roll consequently.

Parameter	Value	Unit
Convergence time	$\tau_y = 15$	[second]
(Error less than 0.5 degree)	$\tau_p = 16$	[second]
	$\tau_r = 15$	[second]
Estimation error mean	$\mu_y = 0.05$	[degree]
(after convergence)	$\mu_p = 0.00$	[degree]
	$\mu_r = 0.01$	[degree]
Estimation error std.	$\sigma_y = 0.14$	
(after convergence)	$\sigma_p = 0.12$	
	$\sigma_r = 0.07$	

A quaternion representation of attitude is used in designing Kalman and information filters. The results are transformed to Euler angles to ease the comparison. The rotation sequence Z-Y-X (or so called 3-2-1) is chosen for the transformations.

Table 1 shows the employed simulation parameters. The first simulation results as shown in Fig. 5 depicts the performance of ADCS while the energy management scheme is deactivated. This result shows that ADCS can successfully meet the determination accuracy requirements while the sensors are used at full rate with the nominal sampling rate.

Table 2 presents different results of attitude estimation in this benchmark scenario. The mean of estimation error is close to zero for yaw, pitch and roll, which shows that the estimation is unbiased and filter is performing as expected. In the next simulations, we have activated our decentralized energy manager scheme (see Algorithm 3). Each node computes the local estimation of the attitude, performs decision

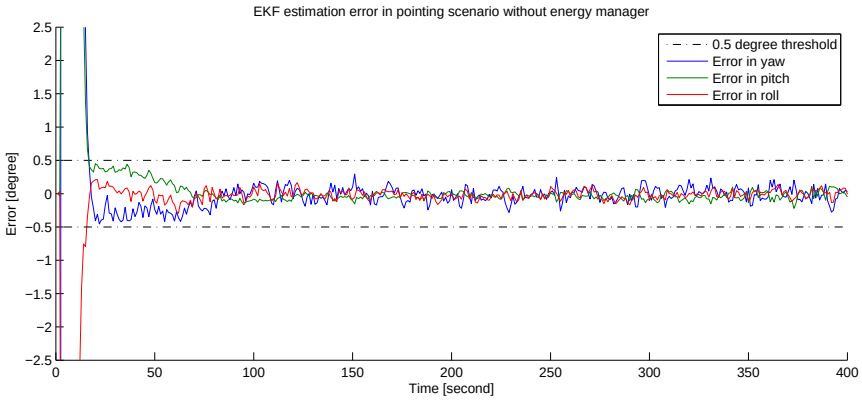

Fig. 5 Simulation result showing the attitude estimation error in pointing scenario.

making based on hypothesis tests, and decides on the necessity of transmitting local measurement vectors. Also we have placed a federated ADCS estimation algorithm on OBC to compare the results of local attitude estimations with the global one. Figures 6, 7 and 8 shows the result of local attitude estimations. Comparing this results with Fig. 9 shows that the ADCS performance on each nodes is quite comparable to the federated result at OBC. Also we can see that all estimators show a quick convergence and meet the ADCS accuracy requirements.

Table 3 presents the characteristics of the local estimators on each node. Similar to the benchmark test, the mean of the estimation residuals are very close to zero which refers to the healthy operation of the estimators. The status of wireless transmitter of nodes are shown in Fig. 10. 'ON' status means that the sensor's wireless transmitter is activated, while 'OFF' means that it is switched to off or sleep mode. In 'ON' mode, the node makes a local measurement vector, establishes a connec-

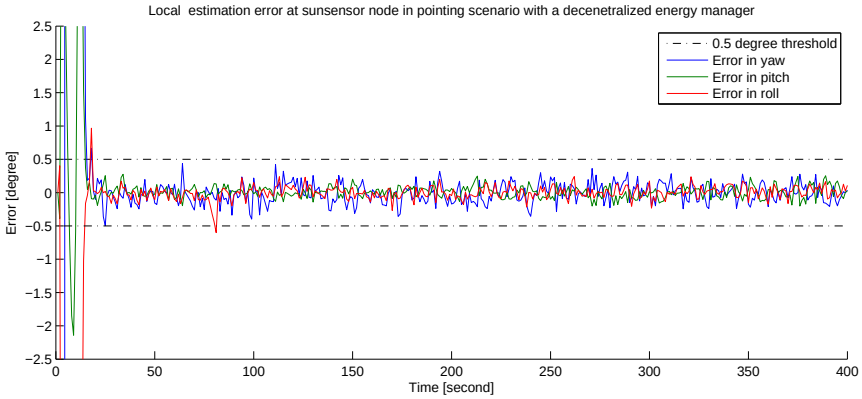

Fig. 6 Simulation results of local attitude determination in sun sensor while decentralized energy manager scheme is operational.

Table 3 Attitude estimation results in pointing scenario with decentralized energy manager. Subscripts *y*, *p* and *r* refer to yaw, pitch and roll, and subscripts *SS*, *MM* and *G* denote sun sensor, magnetometer and gyro, respectively.

Parameter	Value	Unit
Convergence time	$\tau_{SS,y} = 16$, $\tau_{MM,y} = 16$, $\tau_{G,y} = 16$	[second]
(Error less than 0.5 degree)	$\tau_{SS,p} = 15$, $\tau_{MM,p} = 15$, $\tau_{G,p} = 15$	[second]
	$\tau_{SS,r} = 15$, $\tau_{MM,r} = 14$, $\tau_{G,r} = 15$	[second]
Estimation error mean	$\mu_{SS,y} = 0.01$, $\mu_{MM,y} = 0.00$, $\mu_{G,y} = 0.00$	[degree]
(after convergence)	$\mu_{SS,p} = 0.00$, $\mu_{MM,p} = 0.00$, $\mu_{G,p} = 0.00$	[degree]
	$\mu_{SS,r} = 0.00$, $\mu_{MM,r} = 0.00$, $\mu_{G,r} = 0.00$	[degree]
Estimation error std.	$\sigma_{SS,y} = 0.14$, $\sigma_{MM,y} = 0.14$, $\sigma_{G,y} = 0.16$	
(after convergence)	$\sigma_{SS,y} = 0.08$, $\sigma_{MM,y} = 0.07$, $\sigma_{G,y} = 0.07$	
	$\sigma_{SS,y} = 0.09$, $\sigma_{MM,y} = 0.08$, $\sigma_{G,y} = 0.11$	

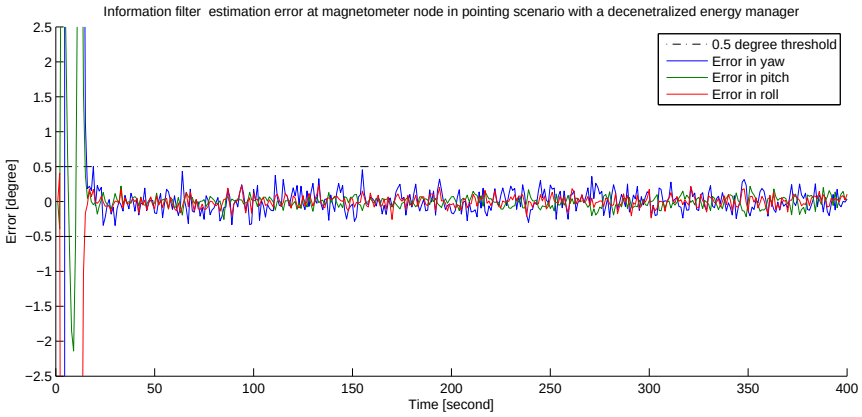

Fig. 7 Simulation results of local attitude determination at magnetometer node while decentralized energy manager scheme is operational.

tion to OBC and transmits the local information vector and local information matrix accordingly. It also receives the relayed information from other sensor nodes. In 'OFF' mode, the local microprocessor continues operation of its information filter without receiving new information vectors from other sensors. We can observe that all sensors are frequently employed during the initial moments of the simulation and then the frequency of activation is remarkably reduced after the convergence of the estimators for two of the sensors. It can be observed that the gyro has been switched to 'OFF' mode during 33.5% of the operation time and the sun sensor has been deactivated for 25.5% of the simulation period. This percentage is about 2.5% for the magnetometer sensor. We can observe that the magnetometer has been more

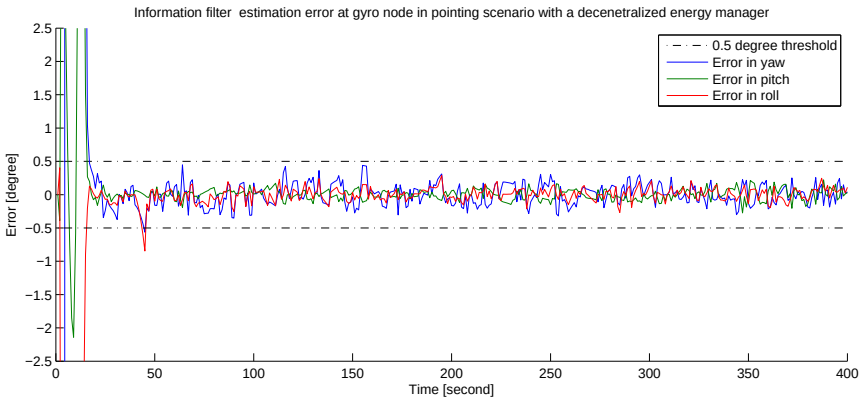

Fig. 8 Simulation results of local attitude determination at gyro node while decentralized energy manager scheme is operational.

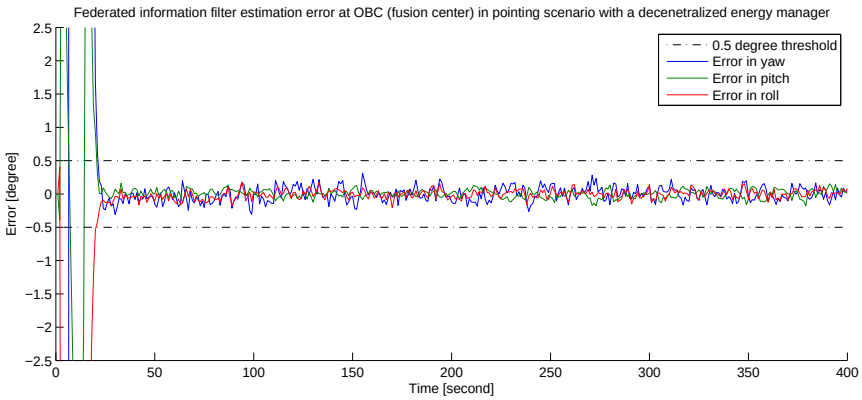

Fig. 9 Simulation result of attitude determination at OBC. A federated information filter is used to produce attitude determination results at OBC for pointing scenario when decentralized energy management scheme is regulating the communication activity of sensor nodes.

frequently activated comparing to the other two sensors. This could be due to noise characteristics of the magnetometer which is relatively high comparing to the other two. We can conclude that by employing more accurate sensors the performance of energy management scheme can be positively affected.

6 Conclusion

In this paper we introduced a decentralized energy management architecture for a spacecraft onboard wireless sensor network. Our decentralized scheme is integrated with the attitude determination system of spacecraft. The proposed approach is based on using decentralized information filter as an estimation method at the sensor nodes. Based on the filtering results, a local energy manager issues the next transmission time to activate the wireless transmitter and send local information to other nodes and the data fusion center. We showed that our energy manager can be realized by using statistical approaches and hypothesis testing. We showed that in a spacecraft pointing scenario, our proposed energy management scheme can reduce the onboard wireless transmission activity which directly reduces the overall energy consumption. The presented simulation results show about 25% to 33% reduction in wireless communication activities of two ADCS sensors which implies a significant improvement in energy efficiency of the sensors.

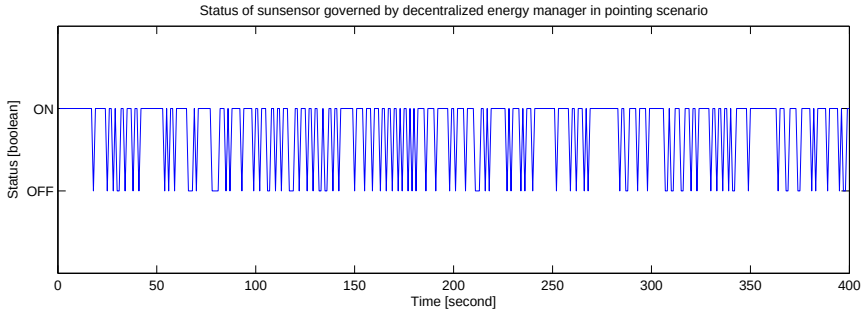

(a) Sun sensor activation status

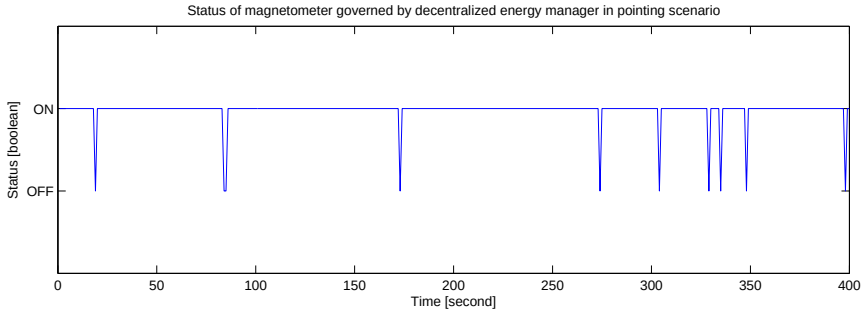

(b) Magnetometer activation status

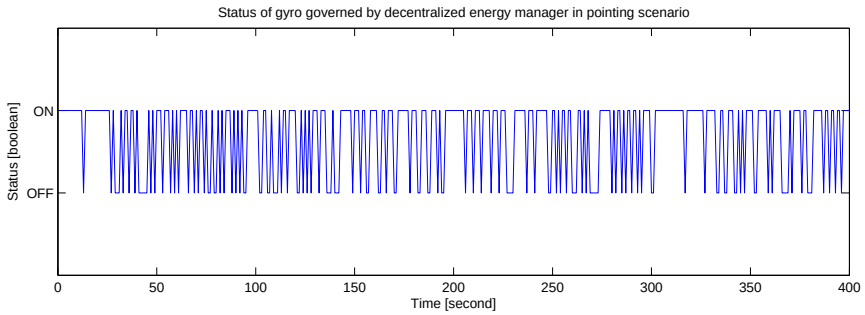

(c) Gyro activation status

Fig. 10 The sensor status are shown here for the first 400 seconds of the simulation.

Acknowledgement

This work is supported by the Dutch Government as part of the decree on subsidies for investments in the knowledge infrastructure (Bsik) program. This work is done within the Micro Satellite (MISAT) project.

References

1. Amini, R., A. Larsen, J. Izadi-Zamanabadi, R., Bhanderi, D.: Design and Implementation of a Space Environment Simulation Toolbox for Small Satellites. Proceedings of 25th International Astronautical Congress, Japan (2005).
2. Amini, R., Gaydadjiev, G, Gill, E.: The Challenges of Intra-Spacecraft Wireless Data Interfacing. Proceedings of IAC Conference, India (2007).
3. Amini, R., Gaydadjiev, G., Gill, E.: Smart power management for an onboard wireless sensors and actuators network. Proceedings of AIAA Space 2009 Conference and Exposition (2009).
4. de Boom, C., Leijtens, J. A. , Duivenbode, L. , van der Heiden, N.: Micro digital sun sensor: System in a package, Proceedings of the 2004 International Conference on MEMS (2004).
5. Eady, F.: Hands-on-Zigbee: Implementing 802.15.4 with Microcontrollers (Embedded Technology). Newnes (2007).
6. Eckerly, S., Schalk, J., Coumar, O., Haira, K.: The EADS micropack. Proceedings of 5th Round table on Micro/Nano Technologies, Noordwijk (2005).
7. Faridani, H. M.: Performance of Kalman filter with missing measurements. Automatica. 22(1) pp. 117–120 (1986).
8. Julier, S.J., Uhlmann, J.K.: Unscented filtering and nonlinear estimation. Proceedings of the IEEE. pp. 401422 (2004).
9. Keshavarzian, A., Lee, H., Venkatraman, L.: Wakeup scheduling in wireless sensor networks. Proceedings of the 7th ACM international symposium on Mobile ad hoc networking and computing, pp. 322-333 (2006).
10. Liu, X., Goldsmith, A.: Kalman filtering with partial observation losses. Proceedings of 43rd IEEE Conference on Decision and Control. 4, pp 4180 – 4186 (2004).
11. Rahimi, M., Baer, R., Iroezi, O., Garcia, J.C., Warrior, Jay, Estrin, D., Srivastava, M.: Cyclops: in situ image sensing and interpretation in wireless sensor networks. Proceedings of the 3rd international conference on Embedded networked sensor systems, pp. 192-204 (2005).
12. Santini, S., Römer, K: An Adaptive Strategy for Quality-Based Data Reduction in Wireless Sensor Networks. Proceedings of the 3rd International Conference on Networked Sensing Systems (INSS06), pp. 29–36 (2006).
13. Sharad, Q.H., Han, Q., Mehrotra, S., Venkatasubramanian, N.: Energy Efficient Data Collection in Distributed Sensor Environments. Proceedings of IEEE ICDCS conference, pp. 590–597 (2003).
14. Silberstein, A., Braynard, R., Yang, J.: Constraint-chaining: On energy-efficient continuous monitoring in sensor networks. Proceedings of SIGMOD conference, pp. 157–168 (2006).
15. Sinha, A., Chandrakasan, A.: Dynamic power management in wireless sensor networks, IEEE Journal of Design Test of Computers, pp. 62–74 (2001).
16. Sinopoli, B., Schenato, L., Franceschetti, M., Poolla, K., Jordan, M.I.,Sastry, S.S.:Kalman filtering with intermittent observations. Proceedings of 42nd IEEE Conference on Decision and Control. 1, pp. 701–708 (2003).
17. Vladimirova, T., Bridges, C., Prassinos, G., Wu, X., Sidibeh, K., Barnhart, D., Jallad, A. H., Paul, J., Lappas, V., Baker, A., Maynard, K., Magness, R.: Characterising wireless sensor motes for space applications. Proceedings of Second NASA/ESA Confrence on Adaptive Hardware and Systems, pp. 43 50 (2007).